

数字全息测量颗粒场研究进展

吴迎春 吴学成 岑可法

(浙江大学能源清洁利用国家重点实验室, 浙江 杭州 310027)

摘要 小颗粒物质在自然界广泛存在且在工业生产中具有重要应用,应用数字全息技术对其进行三维研究具有重要的科学意义及实用价值。系统地对数字颗粒全息技术及其应用进行了综述,具体包括基于光散射理论、衍射理论的颗粒全息图形成及其条纹特性,颗粒全息图的数字重建方法、颗粒识别、定位以及颗粒匹配,数字全息在颗粒场中测量颗粒粒径、三维位置、形貌和三维速度的应用。数字全息作为一种三维测量技术,在颗粒场测量中具有广阔的应用前景。

关键词 全息; 三维重建; 三维位置; 粒径; 三维速度; 形貌

中图分类号 O438.1 **文献标识码** A **doi**: 10.3788/CJL201441.0601001

Development of Digital Holography in Particle Field Measurement

Wu Yingchun Wu Xuecheng Cen Kefa

(State Key Laboratory of Clean Energy Utilization, Zhejiang University, Hangzhou, Zhejiang 310027, China)

Abstract Small particles widely exist in nature, which are applied to various industrial productions. The three-dimensional (3D) characteristics of particles with digital holography play key roles in scientific researches and applications. Digital particle holography and its applications have been systematically surveyed. The formation of particle holography based on light scattering theories and diffraction theories and its fringe patterns are introduced. Holograms processing algorithms including numerical reconstruction, particle detecting, 3D position locating and particle pairing are presented. Typical applications of digital holography to particle field measurement including particle size, shape, 3D position and 3D velocity are demonstrated. Digital holography, as a 3D measurement tool, shows great potential in particle field characterization.

Key words holography; 3D reconstruction; 3D position; particle size; 3D velocity; shape

OCIS codes 090.1995; 100.6890; 120.7250

1 引言

全息术是一种真正的三维照相技术,由 Gabor^[1]于 1948 年发明。全息术包含两个步骤,全息图记录与波前重建。全息图记录是利用光的干涉原理,将携带物体信息的物光波与参考光干涉,通过记录其干涉条纹而记录物光波的振幅与相位。全息图波前重建是利用参考光照射全息图,再现物光波从而重建三维物体。全息图的记录介质从传统的全息干板(胶片)发展到了数字图像传感器。根据记录介质,可以分为光学全息和数字全息。光学全息中,记录介质全息干板(胶片)具有空间分辨率高、参考

光照射瞬态重建等优点,早期被应用到颗粒测量中;同时,光学全息具有后处理复杂等缺点,如需要化学处理显影、三维扫描重建光场等,因而逐步被数字全息取代^[2-3]。数字全息^[4]采用数字记录与数值重建,能够方便地对全息图进行记录、传输、保存、重建及后处理。

小颗粒物质在现代科学与工程中具有广泛存在,如固体颗粒物、液滴、气泡、悬浮颗粒和微生物等^[5]。数字全息技术具有对颗粒场进行三维测量能力,三维定量测量及研究这些颗粒物的粒径^[6]、位置^[6]、速度^[7-10]等信息对许多工业过程具有重要作

收稿日期: 2013-10-15; **收到修改稿日期**: 2014-01-20

基金项目: 国家自然科学基金(51176162)、国家自然科学基金重大项目(51390491)

作者简介: 吴迎春(1986—),男,博士研究生,主要从事多相流和燃烧光学诊断技术方面的研究。

E-mail: wycgsp@zju.edu.cn

导师简介: 吴学成(1978—),博士,副教授,主要从事多相流和燃烧光学诊断技术方面的研究。E-mail: wuxch@zju.edu.cn (通信联系人)

用,如喷雾^[11-14]、燃烧^[15-16]等。因而在颗粒场三维测量中具有重要应用^[17]。

本文系统地对数字颗粒全息技术及其应用进行了简要概述,介绍了基于光散射理论、衍射理论的颗粒全息图形成及其条纹特性,并分析了颗粒全息图处理方法,包括全息图重建方法、颗粒识别及定位,阐述了数字全息在颗粒场中的应用,包括颗粒粒径、三维位置、形貌和三维速度的测量。

2 颗粒全息理论及模拟

2.1 颗粒全息的光散射理论

在数字颗粒全息中,激光照射颗粒场,颗粒散射光作为物光 O ,没有被颗粒散射的光作为参考光 R ,散射光与参考光相互干涉形成颗粒全息条纹,被

CCD 记录为数字全息图,表达式为

$$I_{\text{holo}} = (R + O) \cdot \overline{(R + O)} = R \cdot \bar{R} + O \cdot \bar{O} + O \cdot \bar{R} + R \cdot \bar{O}. \quad (1)$$

颗粒对激光的散射与激光波束和颗粒有关,复杂几何形状的颗粒对激光散射的严格解至今无法求得。颗粒全息中,照射激光束通常为高斯光束。球形均匀颗粒与有形高斯波束的相互作用而形成的颗粒全息可以通过广义米理论(GLMT)来描述^[18-20]。如图 1 所示,考虑笛卡尔坐标系 O_{xyz} 及与之对应的球坐标系 (r, θ, φ) 。束腰半径在 x, y 方向上分别是 ω_{x0}, ω_{y0} 的椭圆激光波束沿 z 轴传播,照射位于 (x_{pn}, y_{pn}, z_{pn}) 的颗粒,CCD 位于 $(r_{\text{ccd}}, \theta_{\text{ccd}}, \phi_{\text{ccd}})$ 。则颗粒对激光的散射光场 $\mathbf{E}_{\text{sca}} = (E_r, E_\theta, E_\phi)$, $\mathbf{H}_{\text{sca}} = (H_r, H_\theta, H_\phi)$ 为

$$\begin{aligned} E_r &= -kE_0 \sum_{n=1}^{\infty} \sum_{m=-n}^{m=+n} c_n^{pw} a_n g_{n,\text{TM}}^m [\xi_n'(kr) + \xi_n(kr)] P_n^{|m|}(\cos \theta) \exp(im\varphi), \\ E_\theta &= -\frac{E_0}{r} \sum_{n=1}^{\infty} \sum_{m=-n}^{m=+n} c_n^{pw} [a_n g_{n,\text{TM}}^m \xi_n'(kr) \tau_n^{|m|}(\cos \theta) + m b_n g_{n,\text{TE}}^m \xi_n(kr) \pi_n^{|m|}(\cos \theta)] \exp(im\varphi), \\ E_\phi &= -\frac{iE_0}{r} \sum_{n=1}^{\infty} \sum_{m=-n}^{m=+n} c_n^{pw} [m a_n g_{n,\text{TM}}^m \xi_n'(kr) \pi_n^{|m|}(\cos \theta) + b_n g_{n,\text{TE}}^m \xi_n(kr) \tau_n^{|m|}(\cos \theta)] \exp(im\varphi), \\ H_r &= -kH_0 \sum_{n=1}^{\infty} \sum_{m=-n}^{m=+n} c_n^{pw} b_n g_{n,\text{TE}}^m [\xi_n'(kr) + \xi_n(kr)] P_n^{|m|}(\cos \theta) \exp(im\varphi), \\ H_\theta &= \frac{H_0}{r} \sum_{n=1}^{\infty} \sum_{m=-n}^{m=+n} c_n^{pw} [m a_n g_{n,\text{TM}}^m \xi_n(kr) \pi_n^{|m|}(\cos \theta) - b_n g_{n,\text{TE}}^m \xi_n'(kr) \tau_n^{|m|}(\cos \theta)] \exp(im\varphi), \\ H_\phi &= \frac{iH_0}{r} \sum_{n=1}^{\infty} \sum_{m=-n}^{m=+n} c_n^{pw} [a_n g_{n,\text{TM}}^m \xi_n(kr) \tau_n^{|m|}(\cos \theta) - m b_n g_{n,\text{TE}}^m \xi_n'(kr) \pi_n^{|m|}(\cos \theta)] \exp(im\varphi), \end{aligned} \quad (2)$$

式中 $c_n^{pw} = \frac{1}{ik} (-1)^n \frac{2n+1}{n(n+1)}$, a_n, b_n 是散射系数, $g_{n,\text{TM}}^m, g_{n,\text{TE}}^m$ 是波束因子, $\pi_n^{|m|}, \tau_n^{|m|}$ 为散射角函数, $\xi_n(kr), \xi_n'(kr)$ 和 $\xi_n''(kr)$ 分别为黎卡提 - 贝塞尔函数函数及其一阶、二阶导数。

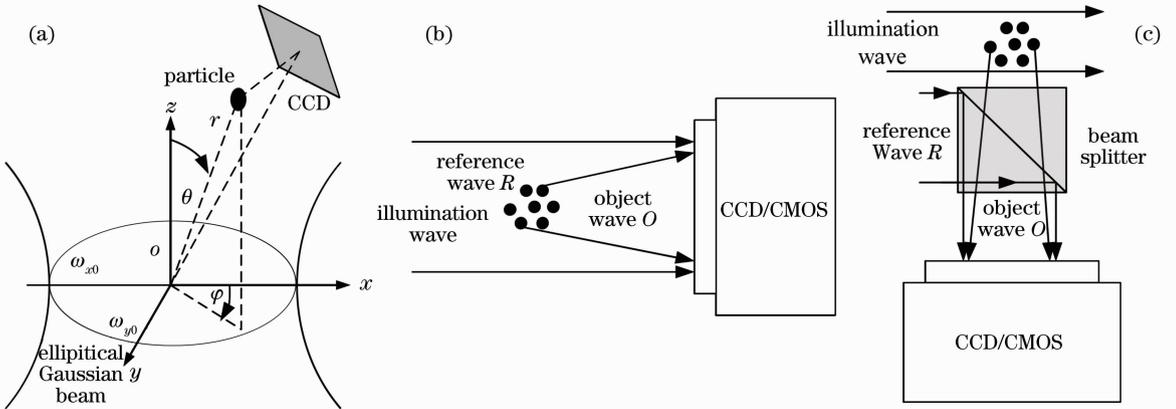


图 1 数字颗粒全息示意图。(a) 椭圆激光波束下颗粒全息示意图; (b) 颗粒同轴全息示意图; (c) 颗粒侧向散射—共轴记录全息示意图

Fig. 1 Sketch of digital particle holography. (a) Particle holography with elliptical Gaussian beam illumination; (b) inline particle holography; (c) side-scattering with inline recording particle holography

当激光波束半径远大于颗粒粒径时,波束可以近似为平面波,波束系数为

$$\begin{aligned} g_n^m &\rightarrow 0, |m| \neq 1, \\ g_{n,\text{TM}}^1 &= g_{n,\text{TM}}^{-1} \rightarrow \frac{1}{2} \exp(ikz_0), \\ g_{n,\text{TE}}^1 &= -g_{n,\text{TE}}^{-1} \rightarrow -\frac{i}{2} \exp(ikz_0). \end{aligned} \quad (3)$$

此时,广义米散射退化为洛伦兹-米散射,颗粒全息可以基于米散射理论来描述^[21-22]。

当颗粒距离 CCD 较远,散射场为远场时,黎卡提-贝塞尔函数存在近似表达式, $\xi_n(kr) \rightarrow i^{n+1} \exp(-ikr)$, 及关系式 $\xi_n''(kr) + \xi_n(kr) = 0$, 因而 $E_r = H_r = 0$ 。在远场散射中,随着无因次粒径参数 $\alpha = \pi d/\lambda$ 的增大,散射光逐渐呈现向前集中的趋势,前向散射光主要是由于颗粒衍射引用的衍射散射光。由于衍射只与颗粒粒径(对于球形不透明颗粒而言)有关,而与颗粒折射率无关。若颗粒折射率 $m \gg 1$, 则颗粒散射系数 a_n, b_n 可以近似为

$$\begin{cases} a_n = b_n = 0.5, & n < \alpha \\ a_n = b_n = 0, & n \geq \alpha \end{cases}. \quad (4)$$

代入平面波颗粒散射公式可求得散射光强为

$$I_s(\theta) = \frac{\lambda^2}{4\pi^2 r^2} I_0 \alpha^4 \left[\frac{J_1(\alpha\theta)}{\alpha\theta} \right]^2, \quad (5)$$

即为颗粒的夫琅禾费衍射光强,表明颗粒全息在远场是物光主要是颗粒衍射光。

在颗粒伽柏同轴全息中,物光为颗粒的前向散射光,参考光即为照射光。在离轴时,物光为颗粒的侧向散射光,参考光可以任意给定。透明颗粒离轴全息中,侧向散射光中的反射光($P=0$)、透射光($P=1$)以及不同阶次的折射光($P=2,3,\dots$)对颗粒全息图的作用可以用洛伦兹-米散射理论的德拜级数来研究^[20,23]。

2.2 颗粒全息的光衍射理论

光散射理论可以严格描述并模拟颗粒同轴及离轴全息图的形成,以及数字颗粒全息系统中各个参数(如激光偏振、颗粒折射率、CCD 位置等)对全息图的影响;但其无穷级数表达对颗粒概念不清晰。应用衍射理论,颗粒全息模型更简单、物理概念更清晰。将球形颗粒看成一个没有厚度的二维不透明圆环,椭圆高斯激光光束照射颗粒上,传播一定距离后到达 CCD。根据 Collins 公式^[24], CCD 上的光场复振幅为

$$\begin{aligned} U(u, v) &= \iint_{-\infty}^{\infty} G_1(x, y) \cdot [1 - T(x, y)] \times \\ &\quad \exp\left[i \frac{\pi}{\lambda B_x} (A_x x^2 - 2ux + D_x u^2)\right] \exp\left[i \frac{\pi}{\lambda B_y} (A_y y^2 - 2vy + D_y v^2)\right] dx dy, \end{aligned} \quad (6)$$

式中 $T(x, y)$ 为颗粒, $T(x, y) = \begin{cases} 1, & \sqrt{x^2 + y^2} \leq d/2 \\ 0, & \sqrt{x^2 + y^2} > d/2 \end{cases}$, $A_{x,y}, B_{x,y}$ 和 $D_{x,y}$ 分别为椭圆高斯激光传播矩阵

$\mathbf{M}_{x,y} = \begin{bmatrix} A_{x,y} & B_{x,y} \\ C_{x,y} & D_{x,y} \end{bmatrix}$ 的元素。积分(6)式的解析解可以精确求得^[25],为了简便,可以对颗粒 $T(x, y)$ 进行复

高斯分解^[26], $T(x, y) = \sum_{k=1}^{10} A_k \cdot \exp\left\{-\frac{B_k[(x-x_0)^2 + (y-y_0)^2]}{r^2}\right\}$ 。光场复振幅 $U(u, v)$ 可以分两项,

$U(u, v) = R(u, v) + O(u, v)$, 式中 $R(u, v), O(u, v)$ 分别为参考光和物光。

$R(u, v)$ 为直接传输到 CCD 表面的波束,仍为椭圆高斯波束

$$\begin{aligned} R(u, v) &= \iint_{-\infty}^{\infty} G_1(x, y) \cdot \exp\left[i \frac{\pi}{\lambda B_x} (A_x x^2 - 2ux + D_x u^2)\right] \exp\left[i \frac{\pi}{\lambda B_y} (A_y y^2 - 2vy + D_y v^2)\right] dx dy = \\ &= \frac{\pi \exp\left[i \left(\frac{\pi D_x}{\lambda B_x} x^2 + \frac{\pi D_y}{\lambda B_y} y^2\right)\right] \exp\left[\frac{\pi^2}{\lambda^2 B_x^2 \left(-i \frac{\pi}{\lambda R_{1x}} - \frac{1}{\omega_{1x}^2} + i \frac{\pi A_x}{\lambda B_x}\right)}\right] x^2 \exp\left[\frac{\pi^2}{\lambda^2 B_y^2 \left(-i \frac{\pi}{\lambda R_{1y}} - \frac{1}{\omega_{1y}^2} + i \frac{\pi A_y}{\lambda B_y}\right)}\right] y^2}{\sqrt{i \frac{\pi}{\lambda R_{1x}} + \frac{1}{\omega_{1x}^2} - i \frac{\pi A_x}{\lambda B_x}} \sqrt{i \frac{\pi}{\lambda R_{1y}} + \frac{1}{\omega_{1y}^2} - i \frac{\pi A_y}{\lambda B_y}}}. \end{aligned} \quad (7)$$

$O(u, v)$ 为椭圆激光光束被颗粒衍射后传输到 CCD 表面的衍射光:

$$O(u, v) = - \iint_{-\infty}^{\infty} G_1(x, y) \cdot T(x, y) \cdot \exp\left[i \frac{\pi}{\lambda B_x} (A_x x^2 - 2ux + D_x u^2)\right] \exp\left[i \frac{\pi}{\lambda B_y} (A_y y^2 - 2vy + D_y v^2)\right] dx dy =$$

$$- \exp\left[i \left(\frac{\pi D_x}{\lambda B_x} x^2 + \frac{\pi D_y}{\lambda B_y} y^2\right)\right] \times$$

$$A_k \pi \exp\left[-\frac{\left(-\frac{i\pi}{\lambda B_x} x + \frac{B_k x_0}{b^2}\right)^2}{\left(-i \frac{\pi}{\lambda R_{1x}} - \frac{1}{\omega_{1x}^2} - \frac{B_k}{r^2} + i \frac{\pi A_x}{\lambda B_x}\right)}\right] \exp\left[-\frac{\left(-\frac{i\pi}{\lambda B_y} y + \frac{B_k y_0}{b^2}\right)^2}{\left(-i \frac{\pi}{\lambda R_{1y}} - \frac{1}{\omega_{1y}^2} - \frac{R_{\text{ell}} B_k}{r^2} + i \frac{\pi A_y}{\lambda B_y}\right)}\right] \exp\left[-\frac{B_k (x_0^2 + y_0^2)}{b^2}\right]$$

$$\sum_{k=1}^{10} \frac{\sqrt{i \frac{\pi}{\lambda R_{1x}} + \frac{1}{\omega_{1x}^2} + \frac{B_k}{r^2} - i \frac{\pi A_x}{\lambda B_x}} \sqrt{i \frac{\pi}{\lambda R_{1y}} + \frac{1}{\omega_{1y}^2} + \frac{R_{\text{ell}} B_k}{r^2} - i \frac{\pi A_y}{\lambda B_y}}}{\sqrt{i \frac{\pi}{\lambda R_{1x}} + \frac{1}{\omega_{1x}^2} + \frac{B_k}{r^2} - i \frac{\pi A_x}{\lambda B_x}} \sqrt{i \frac{\pi}{\lambda R_{1y}} + \frac{1}{\omega_{1y}^2} + \frac{R_{\text{ell}} B_k}{r^2} - i \frac{\pi A_y}{\lambda B_y}}}. \quad (8)$$

CCD 上记录的颗粒全息光强如(1)式。

2.3 颗粒全息的条纹特性

2.3.1 伽柏同轴全息

由(1)式可以看出, $R \cdot \bar{R}$ 和 $O \cdot \bar{O}$ 为分别为参考光和物光的直射光, 不能用来重建颗粒, 颗粒全息的条纹信息包含在干涉项 $O \cdot \bar{R} + R \cdot \bar{O}$ 中。颗粒全息图条纹的形状主要取决于参考光与物光的相互干涉的相位, 由(7)式和(8)式可得

$$\arg(O \cdot \bar{R} + R \cdot \bar{O}) = I \left[\frac{\pi x^2}{\lambda B_x \left(-\frac{\lambda B_x}{\pi \omega_{1x}^2} + i \frac{B_x}{R_{1x}} - i A_x\right)} + \frac{\pi y^2}{\lambda B_y \left(-\frac{\lambda B_y}{\pi \omega_{1y}^2} + i \frac{B_y}{R_{1y}} - i A_y\right)} \right] =$$

$$\frac{\pi x^2}{\lambda B_x R_x} + \frac{\pi y^2}{\lambda B_y R_y} = \frac{\pi x^2}{\lambda z_{x, \text{eq}}} + \frac{\pi y^2}{\lambda z_{y, \text{eq}}}. \quad (9)$$

由(9)式表明, 在椭圆高斯波束下颗粒同轴全息中, 由于纵横象散, 颗粒全息图的等效传播距离在 x, y 方向可以不同, 因而颗粒全息图的二次相位因子的等相位线具有多种形状。图 2 为椭圆高斯激光光束照射下典型颗粒全息图, 全息图的条纹可以为双曲线[图 2(a)]、同心椭圆[图 2(b)]、同心圆[图 2(c)]甚至平行线[图 2(d)]^[19-20, 25, 27-28]。当 $z_{x, \text{eq}}, z_{y, \text{eq}}$ 异号时, 条纹为双曲型, 如图 2(a) 所示; 当 $z_{x, \text{eq}}, z_{y, \text{eq}}$ 同号且不同, 条纹为椭圆型, 如图 2(b) 所示; 当入射波可以近似为平面波或圆形高斯波是, $z_{x, \text{eq}}, z_{y, \text{eq}}$ 相等, 条纹为同心圆, 如图 2(c) 所示; 当 $z_{x, \text{eq}}, z_{y, \text{eq}}$ 同号且相差很大时, 条纹为平行线, 如图 2(d) 所示。

椭圆高斯激光颗粒全息中, 由于等效传播距离可以不同, 因而颗粒全息图的啁啾条纹频率在 x, y 方向也可以不同。以图 2(b) 中的椭圆形条纹为例, 其 x, y 方向条纹如图 3(a) 所示, 发现其条纹频率在 x, y 方向上不同。

颗粒全息图的条纹包含了颗粒的粒径、位置等信息。以入射波为平面波为例, 根据衍射理论, 颗粒全息条纹亮度为^[3, 30]

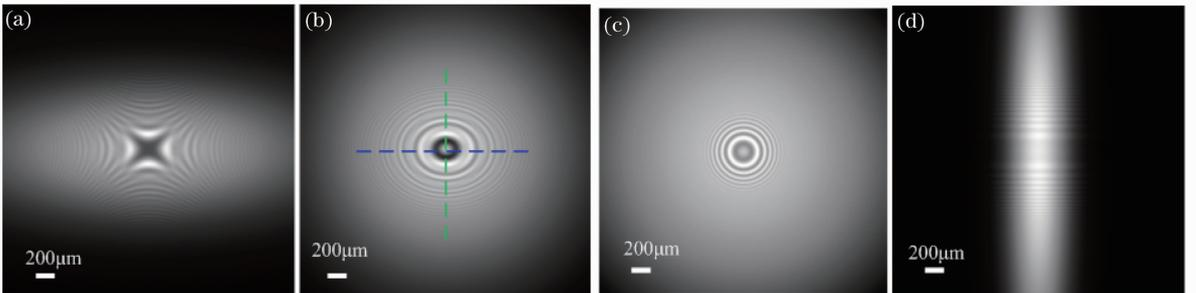


图 2 椭圆高斯激光束照射下典型颗粒全息图。(a) 双曲线型条纹; (b) 同心椭圆型条纹; (c) 同心圆型条纹; (d) 平行线型条纹

Fig. 2 Typical particle holograms with elliptical Gaussian beam illumination. (a) Hyperbolic fringes; (b) elliptical fringes; (c) circular fringes; (d) parallel fringes

$$I(r) = 1 - \frac{2\pi d^2}{\lambda z} \sin\left(\frac{\pi r^2}{\lambda z}\right) \left\{ \frac{2J_1[2\pi dr/(\lambda z)]}{2\pi dr/(\lambda z)} \right\} + \frac{\pi^2 d^4}{\lambda^2 z^2} \left\{ \frac{2J_1[2\pi dr/(\lambda z)]}{2\pi dr/(\lambda z)} \right\}^2. \quad (10)$$

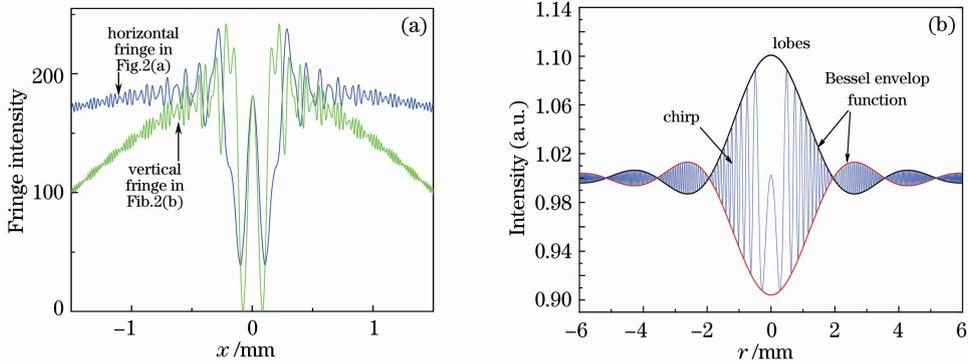


图3 颗粒条纹特性。(a)不同方向上椭圆形条纹特性；(b)平面波照射下同心圆型条纹特性
Fig. 3 Fringes features of particle holograms ion. (a) Elliptical fringes in different directions; (b) circular fringes with plan wave illumination

其条纹为对称的同心圆。图3(b)为球形均匀颗粒在平面波照射下的全息条纹图。颗粒的 z 轴位置包含在啁啾信号 $\sin[\pi r^2/(\lambda z)]$ 中,啁啾信号被贝塞尔函数调制,颗粒的粒径信息包含在这个贝塞尔包络函数中。

2.3.2 颗粒侧向全息

如图1(c)所示,在颗粒侧向全息中,物光是颗粒的侧向散射光^[31-35],参考光可以为任意波束,一般为平面光。对于折射率虚部较大的吸收性颗粒,侧向散射光主要是表面反射光。对于折射率虚部为0(或者很小)的透明颗粒,侧向散射光包含反射光($P=0$)、透射光($P=1$)以及不同阶次的折射光($P=2,3,\dots$)。侧向散射光中的反射光、透射光、折射光可以近似为从颗粒不同位置出射的球面波。这

些球面波与参考光干涉形成颗粒离轴全息图,当参考光为平面光时,颗粒侧向全息图的条纹一般为同心圆环^[20,34-35]。值得注意的是,对于透明颗粒,在近场时,颗粒离轴全息图存在双圆环系统,如图4(c)所示。这主要是由于作为物光的侧向散射光有反射光、透射光、折射光等不同作用的光,且不同阶次的侧向散射光具有不同的出射位置引起的。侧向散射光近似为从颗粒出发的球面波,因而这种侧向全息图的重建图像往往为耀斑,而不是像同轴全息中的颗粒截面形貌。图4(d)~(f)为颗粒离轴全息重建图像,在双圆环中可以得到两个耀斑,分别由反射光、透射光引起的,耀斑距离与颗粒粒径、折射率有关,因而可以用来反演颗粒粒径和折射率等信息^[35]。

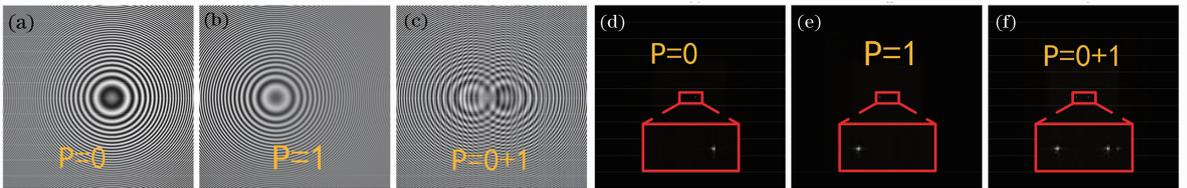


图4 颗粒侧向全息图及其重建耀斑纹特性,颗粒折射率为 $1.33-i0$,侧向散射角度为 90° 。(a)反射光($P=0$)全息图; (b)折射光($P=1$)全息图; (c)双圆环条纹; (d)重建反射耀斑; (e)重建折射耀斑; (f)重建反射、折射双耀斑

Fig. 4 Particle side scattering-inline recording hologram and its reconstructed images, with the particle refractive index of $1.33-i0$ and the recording angle of 90° . hologram with objective wave of (a) reflected wave ($P=0$), (b) refractive wave ($P=1$); (c) two series of concentric rings; (d) reconstructed reflected glare point; (e) reconstructed refracted glare point; (f) reconstructed reflected and refracted glare points

3 数字颗粒全息数据处理

3.1 数字颗粒全息重建

全息重建的基本原理是利用参考光的共轭波照射全息图,从而再现光场复振幅。数字颗粒全息重建方法主要有菲涅耳变换法^[36-37]、卷积法^[28,36]、小波变换法^[38-41]以及分数傅里叶变换法^[27,42-44]。

令 $I_{\text{holo}}(x, y)$ 为全息图, $\bar{E}_{\text{ref}}(x, y)$ 为重建全息图的参考光共轭波, 衍射传播一段距离后得到重建图像 $\Gamma(u, v)$ 为

$$\Gamma(u, v) = \frac{i}{\lambda} \iint I_{\text{holo}}(x, y) \bar{E}_{\text{ref}}(x, y) \frac{\exp\left(-i \frac{2\pi}{\lambda} \rho\right)}{\rho} dx dy, \quad (11)$$

在以平面波作为参考光的情况下, $\bar{E}_{\text{ref}}(x, y)$ 为常数. $\rho = \sqrt{(x-u)^2 + (y-v)^2 + z^2}$ 为传播距离. 在非涅耳近似下 [$z \gg \sqrt{[(x-u)^2 + (y-v)^2]^2 / 8}$], $\rho = \frac{(x-u)^2}{2z} + \frac{(y-v)^2}{2z} + z$, 代入(11)式, 可得

$$\Gamma(\epsilon, \eta) = \frac{i}{\lambda z} \exp\left(-i \frac{2\pi}{\lambda} z\right) \exp[-i\pi\lambda z(\epsilon^2 + \eta^2)] \mathcal{F}^{-1}\left\{I_{\text{holo}}(x, y) \bar{E}_{\text{ref}}(x, y) \exp\left[-i \frac{\pi}{\lambda z}(x^2 + y^2)\right]\right\}, \quad (12)$$

式中根据傅里叶变换, $\epsilon = \frac{u}{\lambda z}$, $\eta = \frac{v}{\lambda z}$. 因而重建得到的图像像素大小为 $\Delta\epsilon = \frac{\lambda z}{N\Delta x}$, $\Delta\eta = \frac{\lambda z}{N\Delta y}$.

根据卷积理论, (11) 式可以看成是 $h(x, y) \bar{E}_{\text{ref}}(x, y)$ 与脉冲响应函数 $g(u, v, x, y) = \frac{i}{\lambda} \frac{\exp\left[-i \frac{2\pi}{\lambda} \sqrt{(x-u)^2 + (y-v)^2 + z^2}\right]}{\sqrt{(x-u)^2 + (y-v)^2 + z^2}}$ 的卷积. 因而可以采用卷积重建

$$\Gamma(u, v) = \mathcal{F}^{-1}\{\mathcal{F}[I_{\text{holo}}(x, y) \bar{E}_{\text{ref}}(x, y)] \cdot \mathcal{F}(g)\}. \quad (13)$$

由于卷积重建方法进行了两次傅里叶变换, 重建图像的像素大小与记录的全息图像像素大小相等, $\Delta u = \Delta x$, $\Delta v = \Delta y$.

波的传播以及衍射过程可以用小波来描述^[45], 因而全息图可以用小波进行重建. 小波具有多尺度重建等优点. 根据小波的构建方法不同, 可以形成不同小波重建方法. Lebrun 等^[38]从线性不变系统出发, 推导了颗粒衍射全息的形成, 构建了相应的小波函数来重建数字颗粒全息图, 并获得了在该方法下重建图像的点扩展函数^[46-47]. Liebling 等^[39]构建了 Fresnellet 小波, 该方法能对全息图进行多尺度重建. Nicolas 等^[27, 42-43]将分数傅里叶光学系统与数字全息进行结合, 应用分数傅里叶变换重建数字全息. 近年来, 新兴压缩感知技术被应用于数字颗粒全息重建^[48].

在一些特殊场合中, 全息图在记录过程中存在像差, 因而在重建过程中需要修正, 如图 5 所示. 如数字显微全息中由于物镜的放大作用产生的球差, 可以通过增加相位因子来修正. 而具有纵横像散的全息图, 可以用在 x, y 方向上用不同的分数阶变换来重建, 也可以在菲涅耳变换重建^[37]、卷积重建^[28, 49]以及小波重建中加入修正因子^[41], 从而消去像散而重建清晰的聚焦颗粒像.

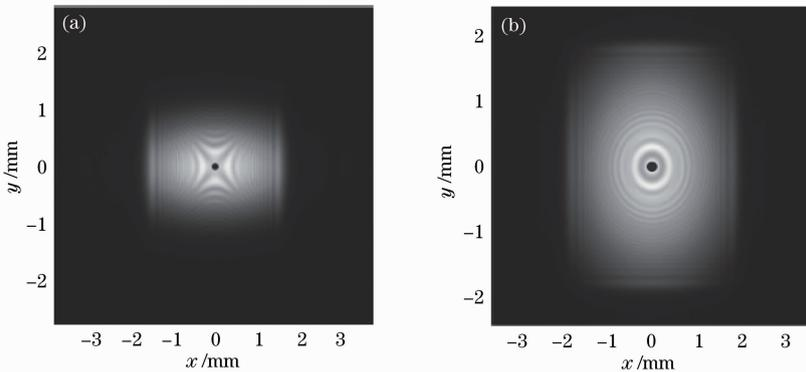


图 5 像散椭圆高斯激光颗粒全息分数傅里叶变换重建图像. (a) 图 2(a) 双曲型条纹颗粒全息图重建图像; (b) 图 2(b) 椭圆形条纹颗粒全息图重建图像

Fig. 5 Reconstructed particle image of astigmatic elliptical Gaussian beam illuminated particle hologram with fractional Fourier transform. (a) Reconstructed image of Fig. 2(a); (b) reconstructed image of Fig. 2(b)

3.2 重建颗粒识别、定位

在重建获得颗粒的三维颗粒光场后, 需要对颗

粒进行识别, 将颗粒从背景中分离出来, 进而获得颗粒的位置、形貌、粒径等信息, 如图 6 所示, 其中“+”

表示第一帧中被识别颗粒的中心,红色轮廓线表示颗粒在第二帧中的轮廓,箭头为颗粒位移方向。重建颗粒可以根据光强、相位与周围环境之间的差异来作为判据进行识别。采用全局阈值^[6]、局部阈值^[50]或自适应阈值^[51]将重建图像二值化,然后将颗粒在二值化图像中进行区域标记识别。在颗粒识别

中,由于激光、流场、颗粒浓度及粒径分布等原因而将噪声识别成颗粒而造成误判,或由于颗粒亮度较低而对颗粒形成漏判。为了减少颗粒误判和漏判,可以采用图像融合等技术,以及综合考虑颗粒的三维光强特性来对颗粒进行识别^[16]。

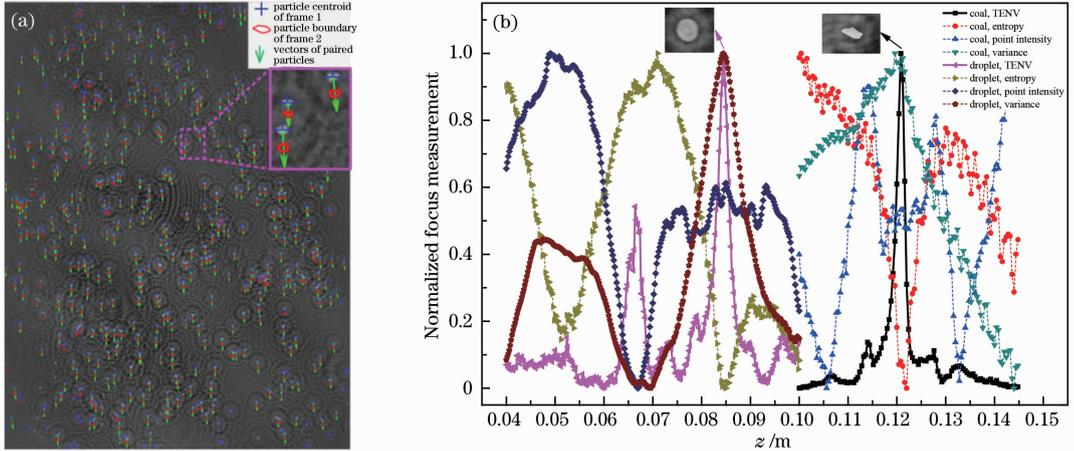


图6 重建颗粒场景深拓展、识别、定位于匹配。(a) 数字全息粒子图像测速技术中拓展景深的重建煤粉颗粒图像;(b) 吸收性非规则煤粉颗粒及透明球形液滴颗粒的 z 轴定位曲线

Fig.6 Extension of depth, detecting, locating and pairing of reconstructed particle field. (a) Extended focus image for particle detecting in digital holography particle image velocimetry; (b) focus metrics of absorbing nonspherical coal particle and transparent spherical droplets

数字颗粒全息的一个关键优势是能对颗粒进行三维定位。颗粒定位的方法主要可以分为空域法、频域法以及空频域法。顾名思义,空域法、频域法以及空频域法分别是在重建图像的空域、频域以及空频域内对颗粒进行 z 轴定位的方法。空域法主要有亮度法^[6,51-52]、亮度方差法^[53-54]、梯度法^[55]、图像熵法^[56]、梯度方差法^[16]、相关法^[57]等。频域法主要是利用图像的傅里叶变换频谱来对颗粒进行定位。空频域法是包括在各种小波变换域^[50,58-59]、分数傅里叶变换域内^[27,42]的颗粒定位方法。颗粒也可以通过多个角度重建图像定位^[60],颗粒 z 轴位置也可以通过条纹分析来确定^[9,58,61]。在实际全息中,由于共轭像等噪声的影响,颗粒全息图的重建率、颗粒识别率、定位精度会受到激光、颗粒浓度、颗粒粒径分布、CCD 分辨率与尺寸等因素的影响。

4 数字颗粒全息应用

数字全息已经被广泛应用到颗粒测量中,包括颗粒几何量测量(包括三维位置、粒径测量、形貌测量)以及运动量(速度)测量。

4.1 颗粒几何量测量

国内外学者对应用数字全息测量颗粒场的三维

位置、粒径分布、颗粒形貌进行了大量研究,被研究的颗粒场包括非规则的固体颗粒^[16,53,60,62]、喷雾液滴^[34,63-65]及气泡^[52,66],甚至包括在火焰中的燃烧着的颗粒及颗粒产物。结合显微技术,数字显微全息可以用来研究微小颗粒,如大小只有几微米的微米颗粒^[67-68]、纳米颗粒^[54,69],甚至大气中的悬浮颗粒^[70-71]。数字显微全息的另一个重要应用是对生物微颗粒进行三维测量,如细胞^[72]、精子^[73]、活体微生物^[74]等。图7为数字全息测量颗粒场几何量典型应用。

4.2 颗粒运动测量

数字全息由于能测量三维位置,因而被用来测量颗粒三维速度,发展为数字全息粒子图像测速(DHPIV)。其测速基本原理是对颗粒场进行多次曝光,从数字全息图中重建不同时刻颗粒三维位置,从而获得颗粒三维速度。在DHPIV中,常见记录方法有双曝光/双帧记录^[32,53,75-77]、多曝光/多帧记录^[78-79]、双曝光/单帧^[80]以及多曝光/单帧^[13]记录。在三维速度场计算方法中,主要有两大类,颗粒跟踪技术及颗粒群三维相关技术。在颗粒跟踪技术中,可以将二维粒子跟踪测速仪(PTV)技术中的最近距离法、匹配概率法^[65,76]、遗传算法^[32,81]等。在三

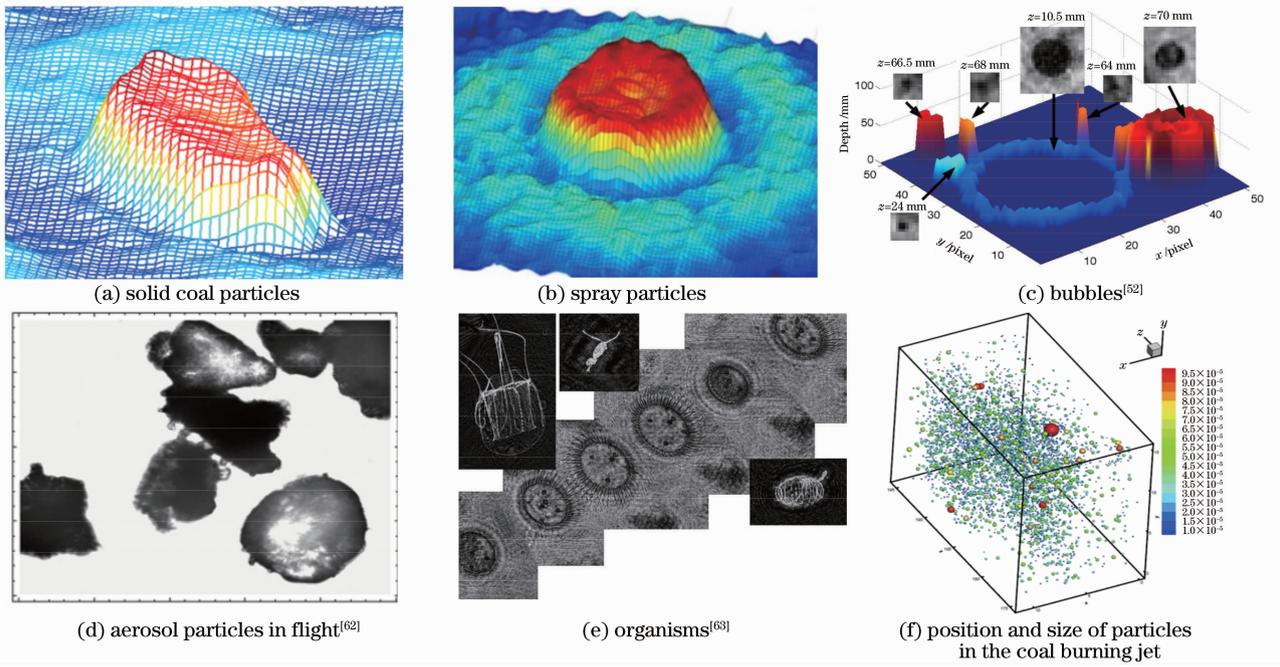


图 7 数字全息测量颗粒场几何量典型应用

Fig. 7 Typical applications of digital holography to measure particle field

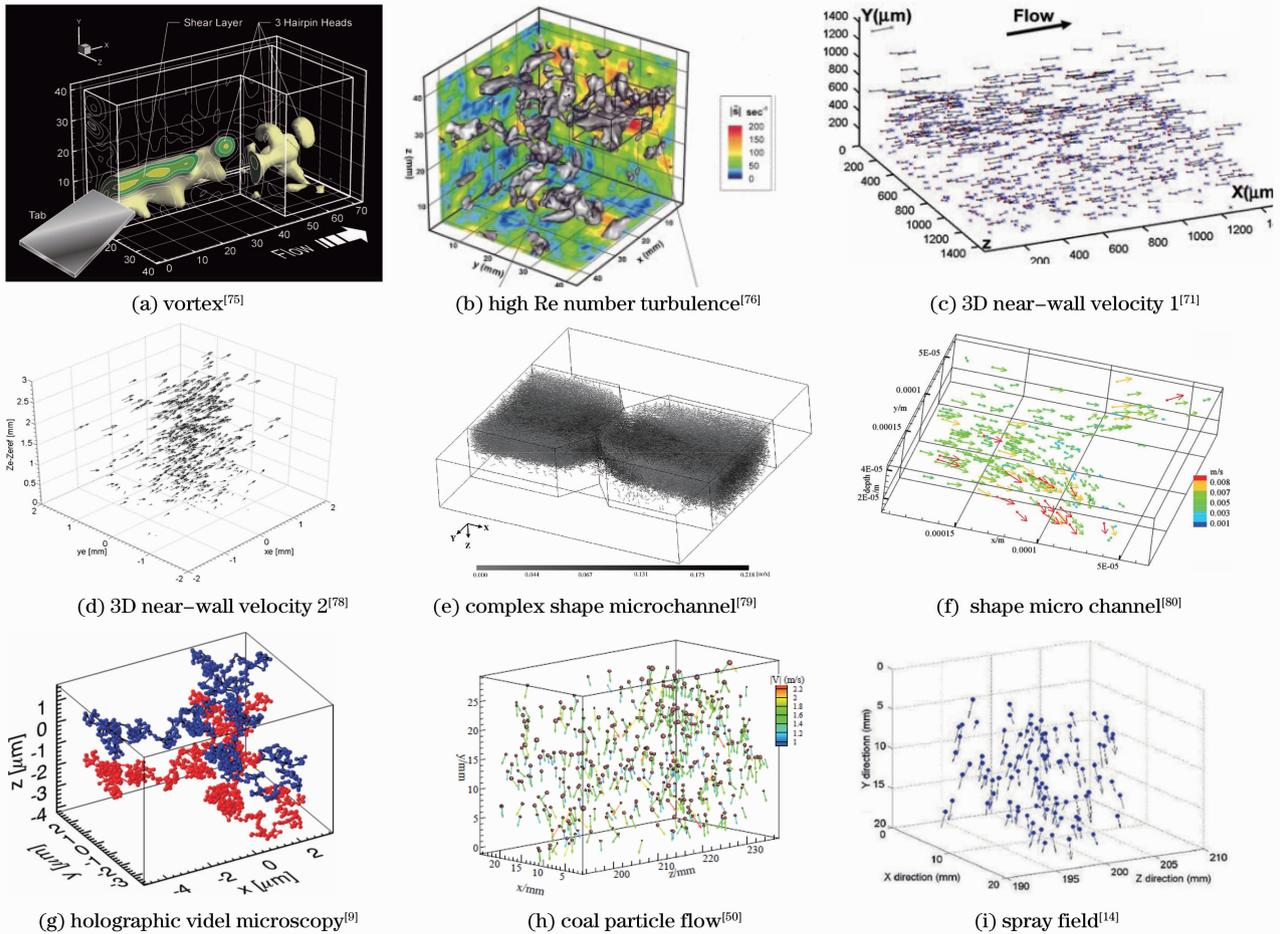


图 8 数字全息测量颗粒场三维运动特性典型应用

Fig. 8 Typical applications of digital holography to measure the 3D motion of particle field

维相关是二维 PIV 互相关的拓展,三维窗口内的两个不同时刻的重建图像进行三维互相关^[82],根据三维互相关的极大值求取颗粒运动位移。

图 8 为数字全息颗粒图像测速在颗粒场三维颗粒流场测量中的典型应用,包括湍流^[83-85]、三维边界层^[75,80]、微流体^[79,86-87]、三维颗粒流^[14,50,53]及生物颗粒流体^[72,88]。Pu 等^[32]建立了 90° 侧向散射 DHPIV 系统,提出了一种基于遗传算法的颗粒匹配方法,开展了一系列湍流三维测量实验^[32,81,83,85,89-90],并将实验结果与粒子图像测速(DNS)模拟结果进行了对比^[85]。Talapatra 等^[66]对高雷诺数的湍流进行了数字全息测量。数字显微全息 PTV 应用到了近壁面处具有大剪切应力及速度梯度的边界层三维测量^[75,80],微流体三维流场测量^[14,50,53]及生物细胞颗粒流体^[72,88]。此外,DHPIV 还可以同时测量颗粒场的三维速度场及粒径,如煤粉颗粒流和喷雾液滴场^[14,50,53]。

5 结 论

数字全息作为一种三维照相技术,具有结构相对简单,实现容易,在颗粒场中具有广泛应用。系统地对数字颗粒全息技术及其应用进行了综述。具体包括基于光散射理论、衍射理论的颗粒全息图形成及其条纹特性,颗粒全息图,重建方法、颗粒识别及定位,数字全息在颗粒场中测量颗粒粒径、三维位置、形貌和三维速度的应用。数字全息作为一种颗粒场三维测量技术,具有广阔的应用前景。

参 考 文 献

- Gabor Dennis. A new microscopic principle[J]. Nature, 1948, 161 (4098): 777-778.
- Meng Hui, Pan Gang, Pu Ye, *et al.*. Holographic particle image velocimetry: from film to digital recording[J]. Meas Sci & Technol, 2004, 15 (4): 673-685.
- Vikram C S, Thompson BJ. Particle Field Holography[M]. Cambridge: Cambridge University Press, 2005.
- Schnars Ulf, Jueptner Werner. Digital Holography: Digital Hologram Recording, Numerical Reconstruction, and Related Techniques[M]. Springer, 2005.
- Cai Xiaoshu, Su Mingxiu, Shen Jiangqi. Particle Size Measurement Techniques and Application[M]. Beijing: Chemical Industry Press, 2010.
- 蔡小舒, 苏明旭, 沈建琪. 颗粒粒度测量技术及应用[M]. 北京: 化学工业出版社, 2010.
- Pu S L, Allano D, Patte-Rouland B, *et al.*. Particle field characterization by digital in-line holography: 3D location and sizing[J]. Exp Fluids, 2005, 39 (1): 1-9.
- Hinsch K D. Holographic particle image velocimetry[J]. Meas Sci & Technol, 2002, 13(7): R61-R72.
- Satake Shin-Ichi, Kunugi Tomoaki, Sato Kazuho, *et al.*. Digital holographic particle tracking velocimetry for 3-D transient flow

- around an obstacle in a narrow channel[J]. Opt Rev, 2004, 11 (3): 162-164.
- Cheong Fook Chiong, Krishnatreya Bhaskar Jyoti, Grier David G. Strategies for three-dimensional particle tracking with holographic video microscopy[J]. Opt Express, 2010, 18 (13): 13563-13573.
- Orlov S S, Abarzhi S I, Oh S B, *et al.*. High-performance holographic technologies for fluid-dynamics experiments[J]. Phil Trans R Soc A: Mathematical, Physical and Engineering Sciences, 2010, 368 (1916): 1705-1737.
- Choo Yeon-Jun, Kang Bo-Seon. Measurements of three-dimensional velocities of spray droplets using the holographic velocimetry system[J]. KSME International J, 2003, 17 (7): 1095-1103.
- Müller J, Kebbel V, Jüptner W. Characterization of spatial particle distributions in a spray-forming process using digital holography[J]. Meas Sci & Technol, 2004, 15(4): 706-710.
- Lü Qieni, Chen Yiliang, Yuan Rui, *et al.*. Trajectory and velocity measurement of a particle in spray by digital holography[J]. Appl Opt, 2009, 48(36): 7000-7007.
- Yang Y, Kang B. Digital particle holographic system for measurements of spray field characteristics[J]. Opt & Lasers in Eng, 2011, 49 (11): 1254-1263.
- Konrath, Konrath R, Schröder, *et al.*. Holographic particle image velocimetry applied to the flow within the cylinder of a four-valve internal combustion engine [J]. Exp Fluids, 2002, 33 (6): 781-793.
- Wu Yingchun, Wu Xuecheng, Zhou Binwu, *et al.*. Coal particle measurement of pulverized coal flame with digital inline holography, in digital holography and 3D imaging[C]. OSA. Kohala Coast, Hawaii United States, 2013. DW3A.3.
- Katz J, Sheng J. Applications of holography in fluid mechanics and particle dynamics[J]. Annual Review of Fluid Mechanics, 2010, 42: 531-555.
- Gouesbet Gérard, Gréhan Gérard. Generalized Lorenz-Mie Theories[M]. Springer, 2011.
- Yuan Y J, Ren K F, Coëtmelec S, *et al.*. Rigorous description of holograms of particles illuminated by an astigmatic elliptical Gaussian beam[C]. J Phys Conf Ser, 2009, 147(1): 012052.
- Wu Yingchun, Wu Xuecheng, Saengkaew Sawitree, *et al.*. Digital Gabor and off-axis particle holography by shaped beams: a numerical investigation with GLMT[J]. Opt Commun, 2013, 305: 247-254.
- Pu Y, Meng H. Intrinsic aberrations due to Mie scattering in particle holography[J]. J Opt Soc Am A, 2003, 20 (10): 1920-1932.
- Wu Xuecheng, Meunier-Guttin-Cluzel Siegfried, Wu Yingchun, *et al.*. Holography and micro-holography of particle fields: a numerical standard[J]. Opt Commun, 2012, 285 (13-14): 3013-3020.
- Li Renxian, Han Xiang'e, Shi Lijuan, *et al.*. Debye series for Gaussian beam scattering by a multilayered sphere[J]. Appl Opt, 2007, 46 (21): 4804-4812.
- Collins J, Stuart A. Lens-system diffraction integral written in terms of matrix optics[J]. J Opt Soc Am, 1970, 60 (9): 1168-1177.
- Verrier Nicolas, Coëtmelec Sébastien, Brunel Marc, *et al.*. Digital in-line holography with an elliptical, astigmatic Gaussian beam: wide-angle reconstruction[J]. J Opt Soc Am A, 2008, 25 (6): 1459-1466.
- Wen J J, Breazeale M A. A diffraction beam field expressed as the superposition of Gaussian beams[J]. J Acoust Soc Am, 1988, 83(5): 1752-1756.
- Nicolas F, Coëtmelec S, Brunel M, *et al.*. Application of the fractional Fourier transformation to digital holography recorded

- by an elliptical, astigmatic Gaussian beam[J]. *J Opt Soc Am A*, 2005, 22 (11): 2569—2577.
- 28 Wu Xuecheng, Wu Yingchun, Yang Jing, *et al.*. Modified convolution method to reconstruct particle hologram with an elliptical Gaussian beam illumination[J]. *Opt Express*, 2013, 21 (10): 12803—12814.
- 29 Verrier Nicolas, Coëtmellec Sébastien, Brunel Marc, *et al.*. Digital in-line holography in thick optical systems; application to visualization in pipes[J]. *Appl Opt*, 2008, 47 (22): 4147—4157.
- 30 Tyler Ga, Thompson B J. Fraunhofer holography applied to particle size analysis a reassessment[J]. *J Modern Optics*, 1976, 23 (9): 685—700.
- 31 Chan K T, Leung T P, Li Y J. Holographic imaging of side-scattering particles[J]. *Opt & Laser Technol*, 1996, 28 (8): 565—571.
- 32 Pu Ye, Meng H. An advanced off-axis holographic particle image velocimetry (HPIV) system[J]. *Exp Fluids*, 2000, 29 (2): 184—197.
- 33 Pu Y, Song X, Meng H. Off-axis holographic particle image velocimetry for diagnosing particulate flows[J]. *Exp Fluids*, 2000, 29 (7): S117—S128.
- 34 Shen H, Brunel M, Coëtmellec S, *et al.*. Glare point reconstruction in digital holographic microscopy for droplet characterization [C]. *Progress In Electromagnetics Research Symposium Proceedings*, 2011, 7(6): 567—570.
- 35 Wu X, Grehan G, Meunier-Guttin-Cluzel S, *et al.*. Numerical investigation of near-field off-axis scattering in-line recording particle holography[C]. *15th Int Symp on Applications of Laser Techniques to Fluid Mechanics*, 2010, 1—9.
- 36 Kreis Thomas. *Handbook of Holographic Interferometry: Optical and Digital Methods*[M]. Wiley-VCH Verlag GmbH & Co. KGaA, 2005. 81—183.
- 37 De Nicola S, Ferraro P, Finizio A, *et al.*. Correct-image reconstruction in the presence of severe anamorphism by means of digital holography[J]. *Opt Lett*, 2001, 26 (13): 974—976.
- 38 Lebrun Denis, Belad Samir, Zkul Cafer. Hologram reconstruction by use of optical wavelet transform[J]. *Appl Opt*, 1999, 38 (17): 3730—3734.
- 39 Liebling M, Blu T, Unser M. Fresnelets: new multiresolution wavelet bases for digital holography[J]. *IEEE Transactions on Image Processing*, 2003, 12(1): 29—43.
- 40 Remacha Clément, Coëtmellec Sébastien, Brunel Marc, *et al.*. Extended wavelet transformation to digital holographic reconstruction; application to the elliptical, astigmatic Gaussian beams[J]. *Appl Opt*, 2013, 52(4): 838—848.
- 41 Wu Xuecheng, Wu Yingchun, Zhou Binwu, *et al.*. Asymmetric wavelet reconstruction of particle hologram with an elliptical Gaussian beam illumination[J]. *Appl Opt*, 2013, 52(21): 5065—5071.
- 42 Coëtmellec Sébastien, Lebrun Denis, Zkul Cafer. Characterization of diffraction patterns directly from in-line holograms with the fractional Fourier transform[J]. *Appl Opt*, 2002, 41(2): 312—319.
- 43 Coëtmellec Sébastien, Lebrun Denis, Zkul Cafer. Application of the two-dimensional fractional-order Fourier transformation to particle field digital holography [J]. *J Opt Soc Am A*, 2002, 19(8): 1537—1546.
- 44 Zhang Y, Pedrini G, Osten W, *et al.*. Applications of fractional transforms to object reconstruction from in-line holograms[J]. *Opt Lett*, 2004, 29(15): 1793—1795.
- 45 Onural L. Diffraction from a wavelet point of view[J]. *Opt Lett*, 1993, 18 (11): 846.
- 46 Malek M, Coëtmellec S, Allano D, *et al.*. Formulation of in-line holography process by a linear shift invariant system; application to the measurement of fiber diameter[J]. *Opt Commun*, 2003, 223 (4-6): 263—271.
- 47 Coëtmellec S, Verrier N, Brunel M, *et al.*. General formulation of digital in-line holography from correlation with a chirplet function [J]. *J European Optical Society-Rapid Publications*, 2010, 5: 10027.
- 48 Wu Yingchun, Wu Xuecheng, Wang Zhihua, *et al.*. Reconstruction of digital inline hologram with compressed sensing [J]. *Acta Optica Sinica*, 2011, 31(11): 1109001. 吴迎春, 吴学成, 王智化, 等. 压缩感知重建数字同轴全息[J]. *光学学报*, 2011, 31(11): 1109001.
- 49 De Nicola Sergio, Finizio A, Pierattini G, *et al.*. Angular spectrum method with correction of anamorphism for numerical reconstruction of digital holograms on tilted planes [J]. *Opt Express*, 2005, 13 (24): 9935—9940.
- 50 Yingchun Wu, Xuecheng Wu, Jing Yang, *et al.*. Wavelet-based depth-of-field extension, accurate autofocusing and particle pairing for digital inline particle holography[J]. *Appl Opt*, 2014, 53(4): 556—564.
- 51 Singh Dhananjay Kumar, Panigrahi P K. Automatic threshold technique for holographic particle field characterization[J]. *Appl Opt*, 2012, 51 (17): 3874—3887.
- 52 Tian L, Loomis N, Dominguez-Caballero J A, *et al.*. Quantitative measurement of size and three-dimensional position of fast-moving bubbles in air-water mixture flows using digital holography[J]. *Appl Opt*, 2010, 49 (9): 1549—1554.
- 53 Wu Y, Wu X, Wang Z, *et al.*. Coal powder measurement by digital holography with expanded measurement area [J]. *Appl Opt*, 2011, 50 (34): H22—H29.
- 54 Sato Akira, Pham Quang Duc, Hasegawa Satoshi, *et al.*. Three-dimensional subpixel estimation in holographic position measurement of an optically trapped nanoparticle[J]. *Appl Opt*, 2013, 52 (1): A216—A222.
- 55 Ilchenko V, Lex T, Sattelmayer T. Depth position detection of the particles in digital holographic particle image velocimetry (DHPIV)[C]. *SPIE*, 2005, 5851: 123—128.
- 56 Chen W, Quan C, Tay C J. Extended depth of focus in a particle field measurement using a single-shot digital hologram[J]. *Appl Phys Lett*, 2009, 95(20): 201103.
- 57 Choo Y J, Kang B S. The characteristics of the particle position along an optical axis in particle holography [J]. *Meas Sci & Technol*, 2006, 17(4): 761—770.
- 58 Soontaranon S, Widjaja J, Asakura T. Extraction of object position from in-line holograms by using single wavelet coefficient[J]. *Opt Commun*, 2008, 281(6): 1461—1467.
- 59 Liebling M, Unser M. Autofocus for digital Fresnel holograms by use of a Fresnelet-sparsity criterion[J]. *J Opt Sci Am A*, 2004, 21(12): 2424—2430.
- 60 Boucherit Sebti, Bouamama Larbi, Benchickh Halim, *et al.*. Three-dimensional solid particle positions in a flow via multiangle off-axis digital holography[J]. *Opt Lett*, 2008, 33(18): 2095—2097.
- 61 Moreno-Hernandez D, Andres B G, *et al.*. 3D particle positioning by using the Fraunhofer criterion[J]. *Opt & Lasers in Eng*, 2011, 49(6): 729—735.
- 62 Darakis Emmanouil, Khanam Taslima, Rajendran Arvind, *et al.*. Microparticle characterization using digital holography[J]. *Chem Eng Sci*, 2010, 65(2): 1037—1044.
- 63 Yang Yan, Kang Boseon. Measurements of the characteristics of spray droplets using in-line digital particle holography [J]. *J Mechanical Science and Technology*, 2009, 23(6): 1670—1679.
- 64 Palero Virginia, Arroyo M, Soria Julio. Digital holography for micro-droplet diagnostics [J]. *Exp Fluids*, 2007, 43(2): 185—195.
- 65 Lü Qieni, Zhao Chen, Ma Zhibin, *et al.*. Digital holography experiment on the measurement of particle size and size distribution of diesel spray[J]. *Chinese J Lasers*, 2010, 37(3):

- 779—783.
吕且妮,赵晨,马志彬,等. 柴油喷雾场粒子尺寸和粒度分布的数字全息实验[J]. 中国激光, 2010, 37(3): 779—783.
- 66 Talapatra S, Sullivan J, Katz J, *et al.*. Application of in-situ digital holography in the study of particles, organisms and bubbles within their natural environment [C]. SPIE, 2012, 8372: 837205.
- 67 Lee Sang-Hyuk, Roichman Yohai, Yi Gi-Ra, *et al.*. Characterizing and tracking single colloidal particles with video holographic microscopy[J]. Opt Express, 2007, 15(26): 18275—18282.
- 68 Wu X, Gréhan G, Meunier-Guttin-Cluzel S, *et al.*. Sizing of particles smaller than 5 μm in digital holographic microscopy[J]. Opt Lett, 2009, 34(6): 857—859.
- 69 Dubois Frank, Grosfils Patrick. Dark-field digital holographic microscopy to investigate objects that are nanosized or smaller than the optical resolution[J]. Opt Lett, 2008, 33(22): 2605—2607.
- 70 Berg M J, Videen G. Digital holographic imaging of aerosol particles in flight[J]. J Quant Spectrosc Radiat Transfer, 2011, 112(11): 1776—1783.
- 71 Abrantes Juliana K, Stanislas Michel, Coudert Sébastien, *et al.*. Digital microscopic holography for micrometer particles in air[J]. Appl Opt, 2013, 52(1): A397—A409.
- 72 Choi Y S, Lee S J. Three-dimensional volumetric measurement of red blood cell motion using digital holographic microscopy[J]. Appl Opt, 2009, 48(16): 2983—2990.
- 73 Caprio G Di, Coppola G, Grilli S, *et al.*. Microfluidic system based on the digital holography microscope for analysis of motile sperm[C]. SPIE, 2009, 7389: 738907.
- 74 Sheng Jian, Malkiel Edwin, Katz Joseph. Digital holographic microscope for measuring three-dimensional particle distributions and motions[J]. Appl Opt, 2006, 45(16): 3893—3901.
- 75 Sheng J, Malkeil E, Katz J. Using digital holographic microscopy for simultaneous measurements of 3D near wall velocity and wall shear stress in a turbulent boundary layer[J]. Exp Fluids, 2008, 45(6): 1023—1035.
- 76 Yang Y, Li G Y, Tang L L, *et al.*. Integrated gray-level gradient method applied for the extraction of three-dimensional velocity fields of sprays in in-line digital holography[J]. Appl Opt, 2012, 51(2): 255—267.
- 77 Li Guangyong, Yang Yan. Digital holography particle image velocimetry applied for measurement of the rotating flow fields [J]. Chinese J Lasers, 2012, 39(6): 0609001.
李光勇,杨岩. 数字全息粒子图像测速技术应用于旋转流场测量的研究[J]. 中国激光, 2012, 39(6): 0609001.
- 78 Satake Shin-Ichi, Kunugi Tomoaki, Sato Kazuho, *et al.*. Three-dimensional flow tracking in a micro channel with high time resolution using micro digital-holographic particle-tracking velocimetry[J]. Opt Rev, 2005, 12(6): 442—444.
- 79 Kim Seok, Lee Sang Joon. Measurement of dean flow in a curved micro-tube using micro digital holographic particle tracking velocimetry[J]. Exp Fluids, 2009, 46(2): 255—264.
- 80 Allano Daniel, Malek Mokrane, Walle Françoise, *et al.*. Three-dimensional velocity near-wall measurements by digital in-line holography: calibration and results[J]. Appl Opt, 2013, 52(1): A9—A17.
- 81 Sheng J, Meng H. A genetic algorithm particle pairing technique for 3D velocity field extraction in holographic particle image velocimetry[J]. Exp Fluids, 1998, 25(5-6): 461—473.
- 82 Shen Gongxin, Wei Runjie. Digital holography particle image velocimetry for the measurement of 3Dt-3c flows[J]. Opt & Lasers in Eng, 2005, 43(10): 1039—1055.
- 83 Pu Ye, Meng Hui. Four-dimensional dynamic flow measurement by holographic particle image velocimetry[J]. Appl Opt, 2005, 44(36): 7697—7708.
- 84 Tao Bo, Katz Joseph, Meneveau Charles. Geometry and scale relationships in high Reynolds number turbulence determined from three-dimensional holographic velocimetry[J]. Phys Fluids, 2000, 12(5): 941—944.
- 85 De Jong J, Salazar J P L C, Woodward S, *et al.*. Measurement of inertial particle clustering and relative velocity statistics in isotropic turbulence using holographic imaging [J]. Int J Multiphase Flow, 2010, 36(4): 324—332.
- 86 Satake S, Anraku T, Kanamori H, *et al.*. Measurements of three-dimensional flow in microchannel with complex shape by micro-digital-holographic particle-tracking-velocimetry [J]. J Heat Transfer, 2008, 130(4): 042413.
- 87 Wu Y, Wu X, Wang Z, *et al.*. Measurement of microchannel flow with digital holographic microscopy by integrated nearest neighbor and cross-correlation particle pairing [J]. Appl Opt, 2011, 50(34): H297—H305.
- 88 Cheong Fook Chiong, Sun Bo, Dreyfus R, *et al.*. Flow visualization and flow cytometry with holographic video microscopy[J]. Opt Express, 2009, 17(15): 13071—13079.
- 89 Meng Hui, Hussain Fazle. Holographic particle velocimetry: a 3D measurement technique for vortex interactions, coherent structures and turbulence[J]. Fluid Dynamics Research, 1991, 8(1-4): 33—52.
- 90 Jones B, Meng H. Nonequilibrium Turbulence Study Using Holographic Particle Image Velocimetry[R]. A087793, 2001.

栏目编辑：何卓铭